Pharm Res (2015) 32:2753–2763
DOI 10.1007/s11095-015-1660-z

RESEARCH PAPER

# EGFR Targeted Theranostic Nanoemulsion for Image-Guided Ovarian Cancer Therapy

Srinivas Ganta • Amit Singh • Praveen Kulkarni • Amanda W. Keeler • Aleksandr Piroyan • Rupa R. Sawant • Niravkumar R. Patel • Barbara Davis • Craig Ferris • Sara O'Neal • William Zamboni • Mansoor M. Amiji • Timothy P. Coleman

Received: 14 November 2014 / Accepted: 18 February 2015 / Published online: 4 March 2015


## ABSTRACT

***Purpose*** Platinum-based therapies are the first line treatments for most types of cancer including ovarian cancer. However, their use is associated with dose-limiting toxicities and resistance. We report initial translational studies of a theranostic nanoemulsion loaded with a cisplatin derivative, myrisplatin and pro-apoptotic agent, $C_6$-ceramide.

***Methods*** The surface of the nanoemulsion is annotated with an endothelial growth factor receptor (EGFR) binding peptide to improve targeting ability and gadolinium to provide diagnostic capability for image-guided therapy of EGFR overexpressing ovarian cancers. A high shear microfludization process was employed to produce the formulation with particle size below 150 nm.

***Results*** Pharmacokinetic study showed a prolonged blood platinum and gadolinium levels with nanoemulsions in *nu/nu* mice. The theranostic nanoemulsions also exhibited less toxicity and enhanced the survival time of mice as compared to an equivalent cisplatin treatment.

***Conclusions*** Magnetic resonance imaging (MRI) studies indicate the theranostic nanoemulsions were effective contrast agents and could be used to track accumulation in a tumor. The MRI study additionally indicate that significantly more EGFR-targeted theranostic nanoemulsion accumulated in a tumor than non-targeted nanoemulsuion providing the feasibility of using a targeted theranostic agent in conjunction with MRI to image disease loci and quantify the disease progression.

S. Ganta • A. Piroyan • R. R. Sawant • N. R. Patel • B. Davis • T. P. Coleman (✉)
Nemucore Medical Innovations, Inc., Worcester, Massachusetts 01608, USA
e-mail: tcoleman@nemucore.com

A. Singh • P. Kulkarni • M. M. Amiji
Department of Pharmaceutical Sciences, School of Pharmacy, Northeastern University, Boston, Massachusetts 02115, USA

P. Kulkarni • C. Ferris
Center for Translational Neuroimaging, Northeastern University, Boston, Massachusetts 02115, USA

S. Ganta • P. Kulkarni • A. Piroyan • R. R. Sawant • N. R. Patel • B. Davis • C. Ferris • M. M. Amiji • T. P. Coleman
Center for Translational Cancer Nanomedicine, Northeastern University, Boston, Massachusetts 02115, USA

S. O'Neal • W. Zamboni
University of North Carolina Lineberger Comprehensive Cancer Center, Chapel Hill, North Carolina, USA

A. W. Keeler • S. O'Neal • W. Zamboni
Division of Pharmacotherapy and Experimental Therapeutics, Eshelman School of Pharmacy, University of North Carolina, Chapel Hill, North Carolina, USA

S. O'Neal • W. Zamboni
Translational Oncology and Nanoparticle Drug Development Initiative ($TOND_2I$) Lab, University of North Carolina at Chapel Hill, Chapel Hill, North Carolina, USA

S. O'Neal • W. Zamboni
Carolina Center of Cancer Nanotechnology Excellence, University of North Carolina at Chapel Hill, Chapel Hill, North Carolina, USA

W. Zamboni
Center of Pharmacogenomics and Individualized Therapy, University of North Carolina at Chapel Hill, Chapel Hill, North Carolina, USA

T. P. Coleman
Blue Ocean Biomanufacturing, Inc., Worcester, Massachusetts 01608, USA

T. P. Coleman
Foundation for the Advancement of Personalized Medicine Manufacturing, Phoenix, Arizona 85013, USA

**KEY WORDS** $C_6$-ceramide · gadolinium · myrisplatin · nanoemulsion · ovarian cancer

## ABBREVIATIONS

| | |
|---|---|
| DNA | Deoxyribonucleic acid |
| EGFR | Endothelial growth factor receptor |
| g | Grams |
| Gd | Gadolinium |
| hrs/h | Hours |
| kg | Kilograms |
| mg | Milligrams |
| min | Minutes |
| mm | Millimeters |
| mmoles | Millimoles |
| msec | Milliseconds |
| mV | Millivolts |
| ng | Nanograms |
| nm | Nanometers |
| psi | Pounds per square inch |
| Pt | Platinum |
| rpm | Revolutions per minute |
| *w/v* | Weight/volume |
| $\mu$L | Microliters |

## INTRODUCTION

Ovarian carcinoma is the most common cause of death from gynecologic malignancy and is frequently associated with a poor outcome due to the difficulties of early diagnosis (1,2). For ovarian cancer, platinum-based drugs—carboplatin and cisplatin—increase overall survival and tumor free survival better than any other chemotherapeutic drug (3). However, their clinical use is still limited due to intrinsic and acquired resistance (4) and generalized toxicity, including acute nephrotoxicity, chronic neurotoxicity and adverse gastrointestinal reactions (5). Recurrent ovarian cancer is classified as been platinum resistant, defined as relapsing within 6 months, or platinum sensitive, defined as relapsing more than 6 months after completing initial platinum-based chemotherapy (6). Treatment decisions based on a cancer being "platinum-sensitive" or "platinum-resistant" underscoring the important role that platinum-based chemotherapy has in the treatment of this disease.

It has been envisioned that use of polymeric conjugates or nanocarrier-based systems may provide improved solubility of platinum-based chemotherapies, prolong half-life in circulation, increase tumor accumulation, decrease non-specific toxicity of platinum-based chemotherapies and potentially reduce the development of drug resistance (7). Thus, various polymeric conjugates and liposomes, micelles, dendrimers, and other carriers have been studied for delivery of platinum compounds (8–11). Cisplatin-loaded liposomes (lipoplatin) reduced tumor burden comparable to cisplatin and showed improved toxicity profile because of the slower release and lower exposure of platinum to normal tissues (12). However, this slower release characteristics also resulted in fewer platinum-DNA abducts from forming thus it was shown to have low clinical advantage over the standard of care platinum therapies (13).

The insolubility of cisplatin in organic solvents and solubility in water pose challenges to encapsulate and control release of platinum-based derivatives in nanomedicines. We recently reported novel hydrophobic platinum-derivatives by attaching myristic acid to cisplatin (myrisplatin) which was encapsulated in the oil core of a stable nanoemulsion (14). Nanoemulsions are colloidal carriers formed by dispersion of oils in water and stabilized with an amphiphilic phospholipid monolayer (15–19). Significant amounts of hydrophobic drug can be loaded in the high volume fraction of the oil core in nanoemulsion (17,19,20). The nanoemulsions we investigate are usually composed entirely of generally regarded as safe grade (GRAS) materials, which have highly favorable safety profiles. Due to their small size (less than 200 nm), nanoemulsions are expected to preferentially accumulate in tumors *via* the enhanced permeability and retention (EPR) effect (21). The surface of the nanoemulsion can be modified with ligands for active targeting to tumors. The usefulness of nanoemulsions to improve delivery of chemotherapeutic payload for the treatment of ovarian cancer has been demonstrated by us (20,22–24).

Theranostic nanomedicines are the state-of the art in molecular design and engineering to develop systems that can be used effectively for the detection, diagnosis, and treatment of cancer. Theranostic nanoemulsions can be engineered to have these capabilities in an all-in-one platform, which include protection and controlled release of a therapeutic payload, targeted delivery and diagnostic functionality. Our nanoemulsions formulations can be surface annotated with gadolinium, a magnetic resonance imaging (MRI) contrast agent and has been shown to have relaxation times comparable to Magnevist® (14,20). Folate-targeted nanoemulsions accumulated in tumors for prolonged period of time compared to Magnevist® and showed enhanced contrast compared to non-targeted nanoemulsions with MRI in SKOV-3 tumor-bearing mice suggesting active targeting of nanoemulsions due to folate modification (20).

In our previous work we developed a novel EGFR-targeted, gadolinium-annotated-theranostic nanoemulsions that co-delivers myrisplatin and $C_6$-ceramide (a proapoptotic agent) which is capable of overcoming platinum resistance *in vitro* and is an effective contrast agent (14). In this paper we describe the initial translational studies articulating imaging, safety, and efficacy capacity of this novel theranostic nanoemulsion.

## MATERIALS AND METHODS

### Materials

A hydrophobic platinum conjugate, myrisplatin was synthesized at the Nemucore Medical Innovations, Inc., (Worcester, MA) using published routes (14,25). Gadolinium chelate gadolinium-diethylenetriaminepentaacetic acid- phosphatidylethanolamine (gadolinium-DTPA-PE) to incorporate into nanoemulsions for MRI functionality was synthesized as described previously (14). EGFR targeting ligand was synthesized as reported previously (14,23). The details regarding synthesis, purification and characterization of these conjugates were reported in our recent publication (14). Cisplatin (*cis*-diammineplatinum (II) dichloride) was from Sigma Chemicals (St. Louis, MO). $C_6$-ceramide (N-hexanoyl-D-erythro-sphingosine) was purchased from Avanti Polar Lipids (Alabaster, AL). Egg phosphotidylcholine (Lipoid® E80) was obtained from Lipoid GmbH (Ludwigshaffen, Germany). The pegylating agent, methoxy-poly(ethylene glycol)-2000 distearoyl-sn-glycero-3-phosphoethanolamine, sodium salt ($PEG_{2000}$DSPE) was purchased from Lysan Bio Inc. (Arab, AL). Poly unsaturated fatty acid (PUFA) rich flax seed oil was received from Puritan's Pride Inc. (Oakdale, NY). All other chemicals and solvents used were of the highest available grade.

### Formulation and Characterization of Theranostic Nanoemulsion

Theranostic nanoemulsion formulation for image-guided therapy consisting of myrisplatin and $C_6$-ceramide in its lipid core and imaging and targeting moieties on the surface was prepared by high shear microfluidization process using LV1 Microfluidizer (Microfluidics Corporation, Newton, MA). The aqueous phase of the formulation was prepared by dissolving egg lecithin (2.4%*w/v*) and $PEG_{2000}$DSPE (0.3%*w/v*) in 4 ml of glycerol (2.21%*w/v*)-water. To which, gadolinium-DTPA-PE (2%*w/v*) and EGFR targeting ligand (0.1%*w/v*) were added and stirred for 1 h to achieve uniform dispersion of all components. Oil phase was prepared by mixing of flax seed oil with the desired amounts of myrisplatin and $C_6$-ceramide dissolved in chloroform, and evaporating the solvent using nitrogen gas, resulting in drug solubilized lipid phase. After this, aqueous and oil phases were heated (60°C, 2 min), mixed and then homogenized at 25,000 psi for 10 cycles to obtain the oil-in-water theranostic nanoemulsion formulations. Non-targeted nanoemulsions were prepared by omitting EGFR targeting ligand from above listed procedure whereas blank nanoemulsions were prepared by omitting EGFR targeting ligand as well as myrisplatin and $C_6$-ceramide.

The platinum concentration in formulations was determined by Inductively Coupled Plasma-Mass Spectrometry (ICP-MS) (14). Gadolinium concentration was monitored by colorimetric method using arsenazo III dye assays as described previously (14,26). $T_1$ relaxation times of gadolinium nanoemulsions formulations were measured using Magnetic Resonance Imaging (MRI). For $T_1$ measurements, nanoemulsion sample in tubes were subjected to a phantom Brucker 500 MHz MRI machine (Bruker Biospec 20/70, Bruker Biospin MRI, Inc, Billerica, MA) in a 4.7 T magnetic field, creating MRI scans showing nanoemulsion generated contrast as well as $T_1$ time measurements. For comparison Magnevist®, a gadolinium-DTPA chelate, was also analyzed for $T_1$ relaxation time at the same gadolinium concentration as the Gadolinium annotated-nanoemulsions.

Size distribution of all nanoemulsion formulations was determined by dynamic light scattering method. For this, samples were diluted 1000 times in deionized distilled water, and the droplet size was determined at 90° angle using Zetasizer ZS (Malvern, UK). Polydispersity index (PDI) was used as a measure for calculating particle size distribution. The zeta potential value of nanoemulsion was also determined using Zetasizer ZS. Nanoemulsion samples diluted in distilled water were placed in electrophoretic cell and the zeta potential measured basing on the electrophoretic mobility of the nanoemulsion droplets.

### Pharmacokinetics and Tissue Distribution

All the animal study protocols were approved by the Northeastern University's Institutional Animal Care and Use Committee. Pharmacokinetics and tissue distribution of platinum and gadolinium were performed in *nu/nu* mice (female, 20–25 g) purchased from Charles River Laboratories (Cambridge, MA). Mice divided into groups having three mice in each group received either intravenous (IV) *via* tail vein or intraperitoneal (IP) administration of non-targeted and EGFR-targeted theranostic nanoemulsions with myrisplatin dose equivalent to 5 mg/kg of platinum. Whereas gadolinium dose was 0.072 mmoles/kg. A group of mice were also administered cisplatin at 10 mg/kg IV vial tail vein. Three mice from each group at various time points (5, 15, 30 min, and 1, 2, 4, 6 and 24 h) were anaesthetized with isoflurane and blood collected from the cardiac puncture into heparin treated tubes. The blood samples were then centrifuged at 3500 rpm for 15 min, the plasma removed and stored at −20°C until analyzed for platinum and gadolinium using ICP-MS at University of North Carolina, Chapel Hill, NC. After blood collection, the mice were euthanized by cervical dislocation, and liver, kidney, heart, lungs and brain were removed. Tissues were stored at −20°C until analyzed for platinum and gadolinium using ICP-MS.

For all treatments, 100 μL of 70% $HNO_3$ with 100 ng/mL of Iridium was added to 50 μL of plasma for sum total metal detection. Samples were digested at 100°C for 90 min. Filtered water was added to make a final volume of 1000 μL for all plasma samples and stored at 4°C until analysis.

For cisplatin samples, tissues were processed to measure total cisplatin as described above. The plasma was processed to measure total and unbound cisplatin. An additional 150 μL of plasma was required for unbound cisplatin concentration detection. Plasma was added to ultracentrifugation chamber and spun at 2500 g for 30 min at 25°C. After centrifugation, 50 μL of ultrafiltration was collected and process like sum total plasma previously described. For tissue sum total gadolinium and Pt detection, a goal weight of 60 to 80 mg was collected. After weight was recorded, 100 μL of 70% $HNO_3$ with 200 ng/mL of Iridium was added to each tissue. Tissues were digested at 100°C for minimum 2 h and filtered water was added for final volume of 2000 μL and stored at 4°C until analysis.

ICP-MS elemental analysis was performed on an Agilent 7500cx (Agilent Technologies, Tokyo, Japan). Instrumental parameters were optimized daily to obtain best sensitivity before analysis. The lower limit of detection for gadolinium, platinum and Iridium was 1.0 ng/mL. Indium was used for the external instrument standard.

### Pharmacokinetic Analysis

Pharmacokinetic parameters of platinum and gadolinium were estimated using WinNonlin (Phoenix version 6.0) program (Pharsight Corporation, USA). The mean residence time (MRT), the volume of distribution (Vd), total body clearance (Cl) and plasma half-life for the elimination phase ($t_{1/2}$) were calculated by non-compartmental analysis (NCA) using weighed least square algorithm with uniform weighing. The area under the plasma and tissue concentration-time profiles (AUC) was calculated by the linear up log down.

### MRI Study

MRI was performed on female *nu/nu* mice (20–25 g) bearing subcutaneous flank SKOV-3 tumors. Female *nu/nu* mice (20–25 g) were injected subcutaneously with $4\times10^6$ SKOV-3 ovarian cancer cells suspended in 100 μL PBS (1:1 ratio of PBS and Matrigel HC) under light isoflurane anesthesia. After the tumor volume reached around 200–300 $mm^3$, the mice were injected ($n=3$) IV *via* tail vein with MRI contrast agent gadolinium at 0.072 mmoles/kg in non-targeted, EGFR-targeted nanoemulsions, or Magnevist®, (a clinically used gadolinium-DTPA chelate) and imaged under MRI over 24 h period using a phantom Brucker 500 MHz MRI machine (Bruker Biospec 20/70, Bruker Biospin MRI, Inc, Billerica, MA) in a 4.7 T magnetic field. MRI scans showing nanoemulsion generated contrast in $T_1$-weighted images was obtained. Magnevist® was used as a clinically relevant control imaging agent compared with nanoemulsions to detect changes in contrast efficiency and/or distribution.

### Therapeutic Efficacy in Tumor Bearing Mice

Female *nu/nu* mice (20–25 g) were injected subcutaneously with $4\times10^6$ SKOV-3 ovarian cancer cells suspended in 100 μl PBS (1:1 ratio of PBS and Matrigel HC) under light isoflurane anesthesia. After the tumor volume reached around 150 $mm^3$, the mice were randomly divided into four groups ($n=6$) and treated with vehicle (Control group), cisplatin solution, non-targeted and EGFR targeted theranostic nanoemulsions on a schedule of every 7 days×5. Treatment groups received first 3 cycles of 5 mg/kg platinum and additional 2 cycles of 7.5 mg/kg platinum. Mice were monitored for tumor growth, survival time and change in body weight following the treatment.

## DATA ANALYSIS

Data are reported as the average and standard deviation. Comparisons between the groups were made using student's *t*-test and with more than two groups, the ANOVA test was used. Values of $p<0.05$ were considered statistically significant.

## RESULTS

### Preparation and Characterization of Theranostic Nanoemulsions

Theranostic nanoemulsion with imaging and targeting functionality, and co-encapsulating myrisplatin and $C_6$-ceramide was prepared using high shear microfluidization process. The oil-in-water formulation was composed of flaxseed oil as an oil core in which myrisplatin and $C_6$-ceramide were solubilized. Flax seed oil was emulsified in a glycerol-water using egg lecithin as an emulsifier. Glycerol was added to the formulation to obtain the osmolality required for IV administration (17). EGFR-targeting ligand and gadolinium-DTPA-PE were dissolved into glycerol-water, and when emulsified into oil, the lipid portion of these conjugates go into the oil core and EGFR and gadolinium remain on the surface of phospholipid monolayer and extends into aqueous phase as described earlier (14). $PEG_{2000}$DSPE was also incorporated in the formulation to reduce mononuclear phagocyte (MNP) based clearance and promote longer blood circulation. Optimized microfludization conditions of 25,000 psi and 10 cycles were

employed to obtain the particle size of formulations below 150 nm with narrow size distribution as reported earlier (14).

Particle size and zeta potential values of the theranostic nanoemulsions are showed in Table I. The mean hydrodynamic particle size of blank, non-targeted and EGFR-targeted formulations was about 150 nm with the PDI below 0.1, suggesting a narrow distribution of particle size in the formulations. Zeta potential measurements of formulations showed a surface charge in the range of −49 to −59 mV. $T_1$ relaxivities were determined using MRI. $T_1$ value of Magnevist® is 22 msec. As seen from Table I, the contrast efficiency of theranostic nanoemulsions is in the close range and comparable to Magnevist®.

## Pharmacokinetics and Tissue Distribution Analysis

The plasma concentration-time curves for platinum and gadolinium after the IV and IP administration of theranostic nanoemulsions and cisplatin are shown in Figs. 1 and 2 with calculated pharmacokinetic parameters reported in Tables II and III. Results show that IV administration resulted in an initial $C_{max}$ for non-targeted and EGFR targeted nanoemulsions, with platinum levels declined slowly over time (Fig. 1) resulting in an observed significantly longer elimination-half lives in mice. Cisplatin also showed an initial $C_{max}$ but blood concentrations of protein bound and elemental platinum cleared at a much faster rate than either nanoemulsion (Fig. 1). Gadolinium blood levels were also declined slowly and tracked with platinum suggesting the gadolinium was not separated out from the formulation in the blood circulation (Fig. 2). This property is important for the nanoemulsion to remain functional for an extended period of time to provide effective tissue contrast by MRI. IP administration showed blood concentrations ($C_{max}$) peaking at 3 h (Tables II and III) and nearly identical levels to IV treated mice for both platinum and gadolinium. $C_{max}$ is not significantly different between non-targeted and EGFR targeted systems for both platinum and Gadolinium levels. However, 2–5-fold difference in $C_{max}$ was observed between IP and IV routes of administration. This difference may be due to nanoemulsion controlling drug release some extent so that the absorption was delayed when delivered through IP route. Overall, the plasma pharmacokinetic profile of platinum was improved when administered in nanoemulsion as compared to cisplatin.

**Table I** Properties of Theranostic Nanoemulsion Formulations

| Formulations | Hydrodynamic diameter of nanoemulsion droplets | | Zeta potential (mV) | T1 relaxivity (msec) |
|---|---|---|---|---|
| | Size (nm) | PDI | | |
| Blank nanoemulsion | 150 ± 2 | 0.01 | −52 ± 10 | – |
| Non-targeted nanoemulsion | 148 ± 6 | 0.05 | −58 ± 11 | 35 ± 14 |
| EGFR-targeted nanoemulsion | 149 ± 3 | 0.06 | −59 ± 13 | 47 ± 1 |

The values are shown as Avg ± SD, $n = 3$

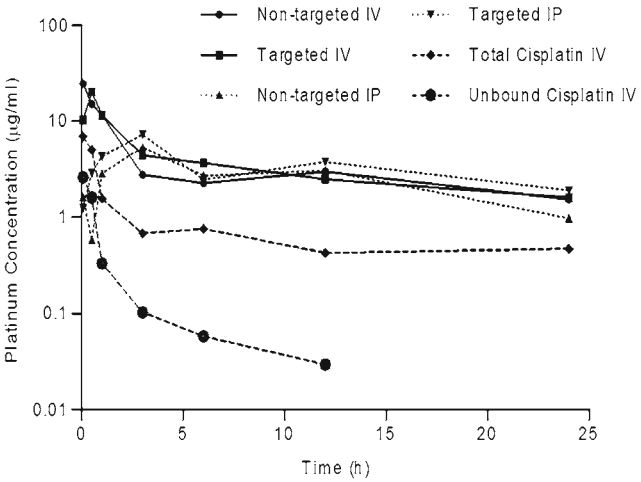


**Fig. 1** Platinum plasma concentration-time profile after IV *via* tail vein or IP administration of cisplatin, non-targeted and EGFR-targeted nanoemulsions to *nu/nu* mice. Myrisplatin dose in nanoemulsion equivalent to 5 mg/kg of platinum and 10 mg/kg for cisplatin. $n = 3$.

Tissue (liver, kidney and lungs) concentrations of platinum and gadolinium after the administration of EGFR-targeted nanoemulsions are shown in Fig. 3. In general significant amounts of platinum and gadolinium levels were noted in liver for nanoemulsions due reticuloendothelial uptake of nanoparticles. After administration of cisplatin the highest exposures occur in the kidney which is consistent with prior studies (27).

## MRI Study

Gadolinium chelates typically provide contrast in tissue compartments in which it is concentrated in T1-weighted images.

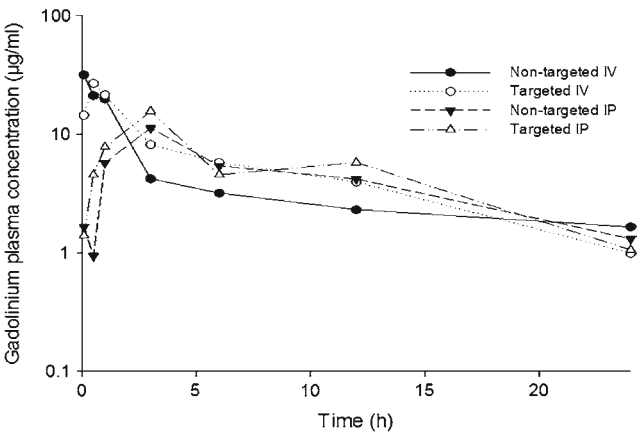


**Fig. 2** Gadolinium plasma concentration -time profile after IV *via* tail vein or IP administration of non-targeted and EGFR-targeted nanoemulsion formulations to *nu/nu* mice. Gadolinum dose was 0.072 mmoles/kg. $n = 3$.

**Table II** Platinum Plasma Pharmacokinetic Parameters After Intraperitoneal (IP) or Intravenous (IV) Administration of Nanoemulsion (NE) Formulations and Cisplatin in *nu/nu* Mice, ($n = 3$)

| Group | Route | $t_{1/2}$ (h) | $T_{max}$ (h) | $C_{max}$ ($\mu$g/mL) | Vd (mL/kg) | Cl (mL/h/kg) | MRT (h) | $AUC_{last}$ (h*$\mu$g/mL) |
|---|---|---|---|---|---|---|---|---|
| Non-targeted NE | IP | 11 | 3.0 | 5.4 | 1021 | 63 | 15 | 63 |
| EGFR-targeted NE | IP | 15 | 3.0 | 7.3 | 889 | 41 | 22 | 81 |
| Non-targeted NE | IV | 12 | 0.08 | 25 | 804 | 46 | 16 | 82 |
| EGFR-targeted NE | IV | 10 | 0.5 | 20 | 657 | 45 | 14 | 86 |
| Cisplatin (total—bound and unbound) | IV | 9.6 | 0.083 | 6.9 | 6752 | 485 | 18.6 | 14 |
| Cisplatin (unbound) | IV | 2.8 | 0.083 | 2.6 | 31,278 | 7776 | 1.7 | 1.2 |

Figure 4a and b shows tumor accumulation of theranostic nanoemulsions following IV injection. Magnevist® rapidly accumulates and clears from the tumor within 6 h, while the non-targeted and EGFR- targeted nanoemulsion accumulate in the tumor for longer duration up to 24 h. However, EGFR-targeted nanoemulsion showed enhanced contrast, suggesting slower clearance rate as compared to non-targeted nanoemulsion. Moreover, the T1-weighted images show that the EGFR-targeted nanoemulsion distributes uniformly across the tumor compared to non-targeted nanoemulsion as well as Magnevist®, Fig. 4a. The relative T1 signal generated by Gd in the tumor region of interest was used to determine uptake. EGFR-targeted nanoemulsion and non-targeted nanoemulsion showed tumor tissue accumulation over the period of 24 h Fig. 4b. The EGFR-targeted nanoemulsion showed enhanced accumulation in tumor tissue compared to non-targeted nanoemulsion. Clinically used magnevist accumulated in tumor tissues very rapidly and cleared within 5 h Fig. 4b. These results indicate the EGFR-targeted theranostic nanoemulsion was effective contrast agent for MRI and the feasibility of using MRI to localize the disease and quantify the disease progression of solid tumors. This data also demonstrates that theranostic nanoemulsions with its payload in the EGFR-targeted nanoemulsion will show a similar accumulation and residence profile in the $EGFR^+$ tumors, which can potentially increase therapeutic efficacy. These results when taken with the pharmacokinetic data showing that platinum and gadolinium have similar clearance profiles suggest that the gadolinium based tumor contrast in MRI (Fig. 4) is a good surrogate marker for platinum accumulation in the tumor.

### Therapeutic Efficacy

The mean survival time was evaluated in mice bearing SKOV-3 ovarian tumors and compared to cisplatin therapy (Fig. 5a). Mice in the control group reached tumor volumes of approximately 1000 $mm^3$ at 21 days, the survival end point for the study, and were removed from the study. However, treated groups survived longer, and the survival times were 21, 25, 32 and 32 days with control, cisplatin, non-targeted and EGFR-targeted nanoemulsions, respectively. Mice were administered with 5 mg/kg of Pt on every week for three weeks, later the dose was increased to 7.5 mg/kg based on tumor response and continued for 4th and 5th week. Toxic effects in cisplatin treated mice were evident, as mice lost 20% of their body weight and were sacrificed (Fig. 5b). However, the mice in the non-targeted and EGFR-targeted theranostic nanoemulsion groups did not lose significant weight and their physical activity was normal. These results suggest that mice tolerated a high dose of Pt given in the nanoemulsion formulations.

## DISCUSSION

Recurrent cancers develop multidrug resistance (MDR) to conventional and novel chemotherapeutic agents representing a formidable challenge in clinical cancer therapy, especially for the effective treatment of gynecological malignancies, which are generally diagnosed at a late stage. Ovarian cancer is the most lethal of the gynecologic cancers due to its

**Table III** Gadolinium Plasma Pharmacokinetic Parameters After Intraperitoneal (IP) or Intravenous (IV) Administration of Nanoemulsion (NE) Formulations in *nu/nu* Mice, ($n = 3$)

| Group | Route | $t_{1/2}$ (h) | $T_{max}$ (h) | $C_{max}$ ($\mu$g/mL) | Vd (mL/kg) | Cl (mL/h/kg) | MRT (h) | $AUC_{last}$ (h*$\mu$g/mL) |
|---|---|---|---|---|---|---|---|---|
| Non-targeted NE | IP | 8.5 | 3 | 11 | 1142 | 93 | 12 | 106 |
| EGFR-targeted NE | IP | 7.7 | 3 | 16 | 894 | 80 | 10 | 130 |
| Non-targeted NE | IV | 8.7 | 0.08 | 32 | 1185 | 94 | 12 | 99 |
| EGFR-targeted NE | IV | 5.9 | 0.5 | 27 | 696 | 81 | 8 | 131 |

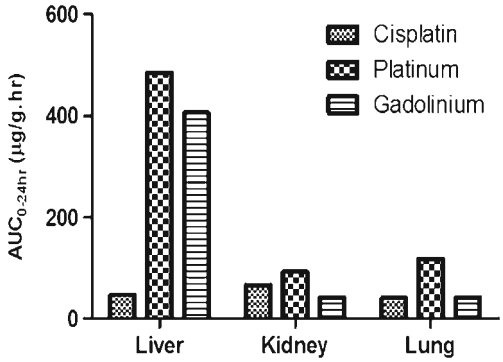


**Fig. 3** Free Cisplatin and platinum, gadolinium levels in tissues after IV administration *via* tail vein in *nu/nu* mice. Cisplatin dose was 10 mg/kg. EGFR-targeted nanoemulsion were administered at myrisplatin dose equivalent to 5 mg/kg of platinum and 0.072 mmoles/kg of gadolinium. $n = 3$.

propensity to spread into the upper abdomen and beyond, and a majority of newly diagnosed ovarian cancer patients will progress to a chemo-resistant state. Platinum containing therapeutic compounds are alkylating agents that exert anticancer activity by disrupting DNA structure in cell nuclei through the formation of intrastrand and interstrand cross-links (28–30). Cisplatin is used to treat ovarian cancer patients, but there is significant dose related nephrotoxicity. Carboplatin, which has virtually replaced cisplatin for patient treatment, forms reactive species more slowly than cisplatin and has a much better, but still significant, toxicity profile including renal damage, electrolyte loss, nausea and vomiting.

Toxicity and platinum-resistance are the driving force to identify safer, more effective and selective platinum therapy.

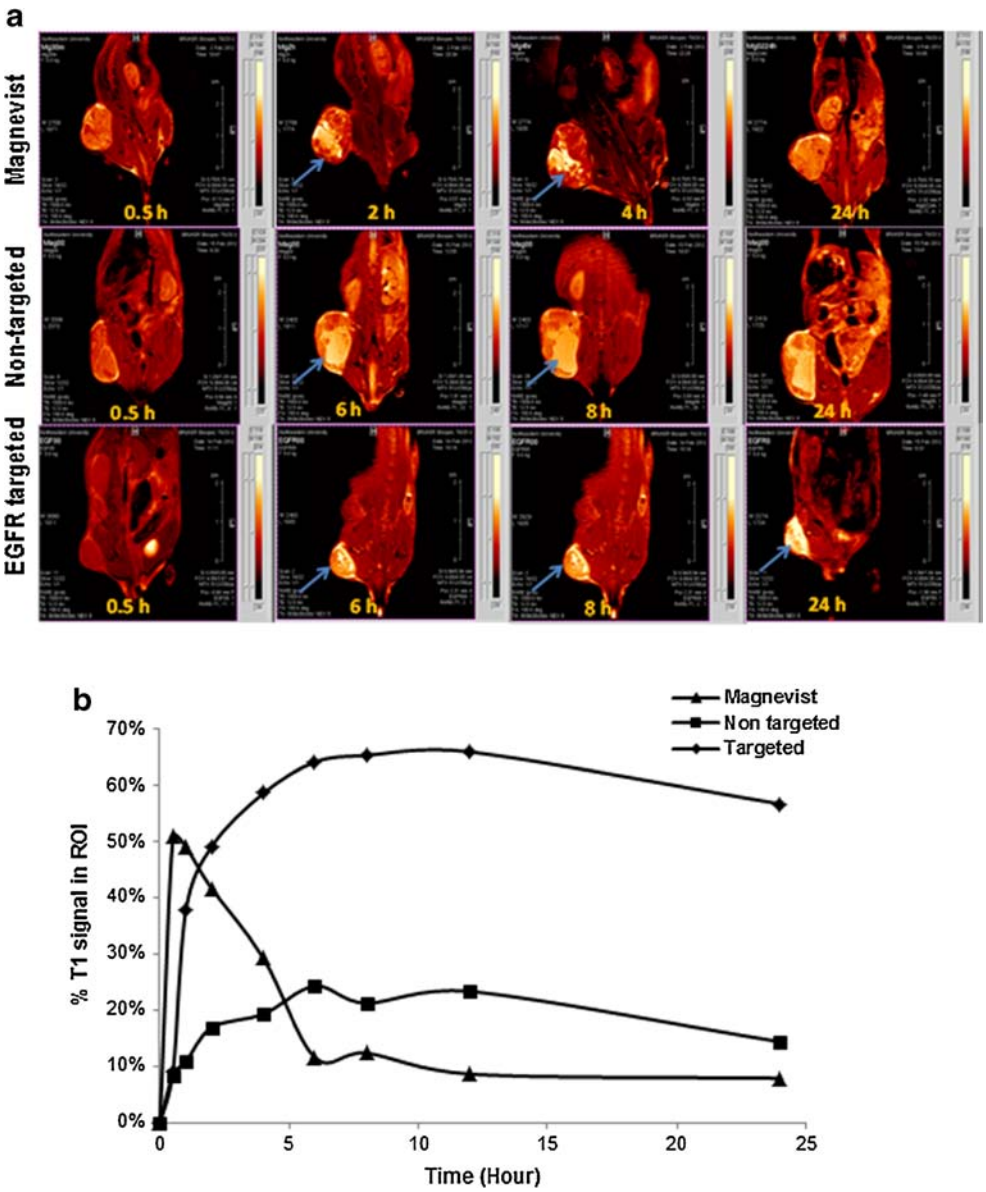


**Fig. 4** (**a**) T1 weighted MR images and (**b**) quantitative analysis of % tumor signal vs time of mice bearing subcutaneous SKOV-3 tumor xenograft post IV injection *via* tail vein of magnevist, non-targeted nanoemulsion and EGFR-targeted nanoemulsion. *Arrows* indicate accumulation of gadolinium in tumor tissue. $n = 3$.

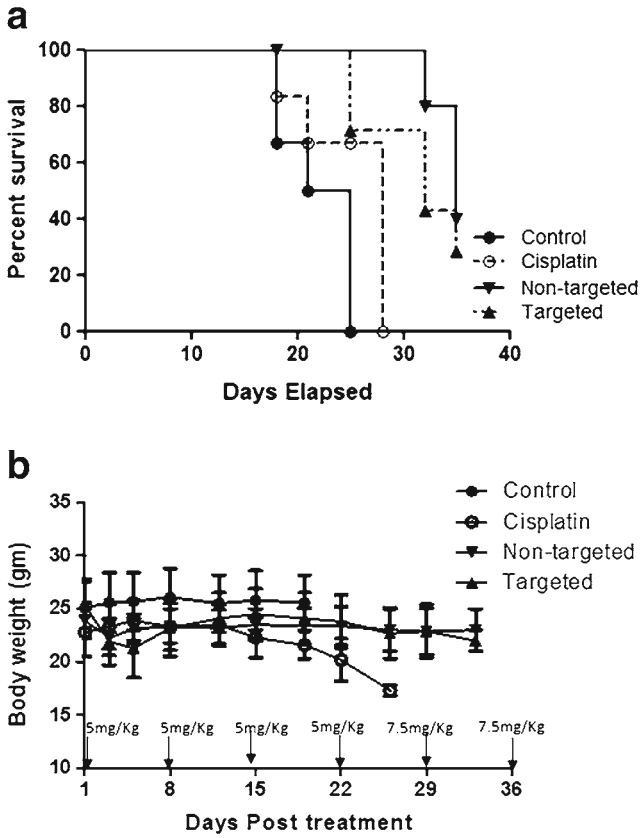


**Fig. 5** (**a**) Kaplan-Meier survival analysis and (**b**) change in body weight on *nu/nu* mice bearing SKOV-3 ovarian tumors when injected with vehicle control, cisplatin alone, myrisplatin and $C_6$-ceramide loaded non-targeted and EGFR-targeted theranostic nanoemulsions IV *via* tail vein. $n = 6$, ±S.D.

Strategies include preparing hydrophobic prodrugs, platinum-polymer conjugates or encapsulating them into nanocarrier formulations for targeted and controlled release (31–33). Lipoplatin, a cisplatin liposomal formulation, was tested in phase I–III clinical trials, and showed a significantly improved toxicity profile and a reduction in tumor burden comparable to that of free cisplatin but overall it has not proven to be more efficacious (12,34). STEALTH liposomal cisplatin formulations were developed for the treatment of cancers that are generally sensitive to platinum, but may be resistant to conventional cisplatin, and reduce toxicities by preferentially delivering drug to the tumor. Even though there is a several-fold higher exposure of total Pt in tumors compared to cisplatin, this did not translate into significant antitumor response in clinical trials (13,35). These results suggest that formulations distribute into tumors, but release less platinum and form fewer platinum-DNA adducts than cisplatin (13).

Innovation in platinum encapsulation and controlled release are still a challenge due to physicochemical properties of platinum compounds. Lipophilicity is a critical parameter for design of novel platinum-based drugs to improve absorption and transport through membranes (36). In a recent study, a platinum prodrug was synthesized that had enough hydrophobicity for encapsulation in PLGA-b-PEG nanoparticles, which was found to be safe and effective (31). Recently platinum compounds containing a monocarboxylate and O ->Pt complexation resulted in a faster release of DNA reactive adducts comparable to cisplatin (33), and formed the basis for designing some lipophilic platinum derivatives suitable for nanoemulsion encapsulation. In this paper, we report initial *in vivo* data of a theranostic nanoemulsion with a cisplatin derivative, myrisplatin and pro-apoptotic agent, $C_6$-ceramide for image-guided therapy of EGFR overexpressing ovarian cancer.

Our strategy for platinum therapy focuses on the development of lipophilic platinum conjugates that can be incorporated into the oil core of long-circulating targeted nanoemulsions. Our platinum chemistry involves the synthesis of hydrophobic platinum tailed with a myristic acid. Another reason for encapsulation of platinum in a nanoemulsion is to design additional features into the delivery system that could assist in mitigating platinum-resistant mechanisms. Mechanisms of platinum resistance include: reduced platinum influx, increased platinum efflux, escape from apoptosis, sequestration by chemical conjugation, or increased DNA repair (37). The present nanoemulsion is designed to enhance platinum influx by receptor-mediated endocytosis, potentially reduce platinum efflux and diminish escape from apoptosis.

Tables II and III highlights the enhanced pharmacokinetic profile of platinum/gadolinium delivered by either targeted or non-targeted nanoemulsions administered either IV or IP All parameters suggest the both formulations are long circulating and remain intact. Notably there is a significant increase in half life of the platinum/gadolinium compared to cisplatin. The biodistribution profile of platinum and gadolinum was also comparable. The nanoemulsion mainly accumulated in liver which is the common elimination pathway for nanocarriers (Fig. 3). Even though still consistent with long-circulation, we also observed a difference in the half life of gadolinium compared to platinum in the nanoemulsions. We attribute this difference to the way the nanoemulsions were designed to have the gadolinium-DTPA chelating moiety exposed on the surface so it could function as contrast agent while myrisplatin is sequestered inside the oil droplet to abrogate platinum binding to serum protein to mitigate systemic toxicities. The gadolinium chelation mechanism with DTPA-PE conjugate includes a coordination with a free water molecule which could be responsible for premature release of gadolinium from the particle and difference in half life exhibited by these formulations. .

Encapsulation of the prodrug, myrisplatin, in the lipid core of the nanoemulsion protects the platinum from the elemental platinum-efflux mechanisms. To enhance influx the surface of the nanoemulsion was functionalized with an EGFR binding peptide, which preferentially binds with high affinity to the

EGF receptor and undergoes receptor-mediated endocytosis of the targeted nanoemulsion. In light of the correlation with poor clinical outcome we previously investigated whether targeting EGFR could enhance *in vitro* potency (14). EGFR targeting was achieved through the use of a lipidated-version of a 12 amino acid peptide that has demonstrated efficient binding and preferential internalization into EGFR over expressing tumor cells *in vitro*, and tumor xenografts *in vivo* (23,38–40). Our previous study found that EGFR targeting enhanced the potency of myrisplatin as compared to the non-targeted approach (14).

We examined the ability of the platinum carrying nanoemulsions to limit tumor growth of SKOV-3 cells *in vivo*. Non-targeted and EGFR-targeted nanoemulsions were used for the first time to deliver myrisplatin in combination with ceramides and slowed tumor growth comparable to cisplatin at equal doses. From our knowledge of the STEALTH liposomal cisplatin studies where platinum had difficulties releasing from the liposomes, we designed our *in vivo* efficacy experiment to directly compare equal doses of nanoemulsion encapsulated platinum to cisplatin. If we did not see any efficacy with this design then it might indicate nanoemulsion encapsulated myrisplatin was not releasing platinum to form DNA-platinum adducts. However, during our *in vivo* study we found that both targeted and non-targeted nanoemulsions had similar effects on growth of SKOV-3 xenograft tumors (data not shown) and improved survival compared to the cisplatin control group. Figure 5a shows that median survival for groups treated with non-targeted and targeted nanoemulsions was significantly different from control; while the cisplatin itself did not differ significantly from control. The dose escalation phase of the study indicated that non-targeted and EGFR-targeted nanoemulsions did not induce the significant weight loss which the cisplatin cohort experienced. This indicates a potential for widening the therapeutic window for platinum therapies, since myrisplatin encapsulated nanoemulsions had significantly less systemic toxicity Fig. 5b. The results indicate that therapeutic platinum is being released but EGFR-targeting is not improving efficacy in this initial assay which is counter intuitive given the results of the MRI study and needs to be investigated further.

A key challenge in ovarian cancer diagnosis and therapy is the ability to follow drug pharmacodynamics within the tumor region in real time. The nanoemulsions created for this study was designed as a theranostic, capable of simultaneously imaging and targeting drug delivery to EFGR-positive ovarian tumors. We designed our platinum-delivery vehicle so a relative imaging signal indicative of nanoemulsion uptake by a tumor shortly after IV injection and in a non-invasive manner by functionalizing the surface of the nanoemulsion with gadolinium-DTPA-PE chelate containing paramagnetic ion gadolinium for MRI contrast enhancement. This design with the gadolinium chelate residing on the outer surface of the nanoemulsion provides a suitable environment for gadolinium longitudinal relaxivity and generates contrast for MRI, thus allowing rapid visualization of drug pharmacodynamics and potentially quicker monitoring of disease progression in ovarian cancer patients.

Previously we showed that non-targeted and targeted nanoemulsions have T1 values similar to those seen for clinically approved Magnevist®. We investigated whether nanoemulsion has the ability to effectively target subcutaneous $EGFR^+$ SKOV-3 cells and enhance the T1 signal of the tumor. SKOV-3 tumors were grown to 200–300 $mm^3$, and serially imaged over 24 h. Figure 4a images show the resulting data of the entire mouse. Magnevist® rapidly accumulates in the tumor over the first hour and resolves to near baseline by the 6th hour. Non-targeted nanoemulsion primarily accumulates by the EPR effect enhancing tumor imaging over a longer period of time than Magnevist®. Targeted nanoemulsion takes advantage of both the EPR effect and active targeting of $EGFR^+$ SKOV-3. EGFR-targeted nanoemulsions accumulate faster and have a longer resident time in the tumor than the other agents. This data suggest the therapeutic platinum/$C_6$-ceramides should have a longer resident time in the tumor increasing the potential for a therapeutic response. Further investigations will have to be performed to understand the perceived differences between the efficacy and imaging studies.

Overall, this study demonstrates that the theranostic properties of a targeted platinum nanomedicine should be advantageous for the treatment of highly aggressive EGFR-positive ovarian cancer. As most ovarian cancers will eventually become platinum-resistant we have shown that co-delivery of myrisplatin and $C_6$-ceramide provides a potential therapeutic option that is less toxic and has attributes designed to overcome platinum resistance by using receptor-mediated endocytosis to enhance particle accumulation as shown by MRI. The diagnostic potential of the nanoemulsion is designed for direct monitoring of nanomedicine tissue distribution and has potential for monitoring disease progression.

## CONCLUSIONS

We developed a multifunctional nanodelivery platform consisting of the theranostic nanoemulsion with a cisplatin derivative, a novel platinum compound myrisplatin and pro-apoptotic agent, $C_6$-ceramide targeted with EGFR biding peptide and gadolinium for diagnostic capability. The formulation was effective and less toxic than cisplatin in treating a xenograft ovarian cancer model. These theranostic nanoemulsion formulations can be delivered at the same or greater dose than cisplatin and Magnevist® with no visual signs of toxicity. It will be interesting to see if distribution of imaging agent can be used to predict distribution of

therapeutic agent and thereby can be used to predict therapeutic response in patients. This would be an important advancement in the treatment of platinum-resistance as physicians have a limited opportunity to find an effective therapy for patients with such advanced disease. While further preclinical efficacy, imaging and toxicology investigations are required to confirm these results, the medical utility of this novel nanomedicine configuration based on the initial results is promising.

## ACKNOWLEDGMENTS AND DISCLOSURES

This study was supported by the NIH grants (R43 CA144591 and U54 CA151881). The Authors would like to thank Susan Riley Keyes, Allison Morse, Samantha Orosz, Laurie Cote, Phil Heisler and Keri Forbringer for their insightful discussion of the findings and assistance with development of this manuscript.

## REFERENCES

1. Siegel R, Naishadham D, Jemal A. CA Cancer J Clin. 2013;63(1):11–30.
2. Jelovac D, Armstrong DK. Recent progress in the diagnosis and treatment of ovarian cancer. CA Cancer J Clin. 2011;61(3):183–203.
3. Neijt JP, ten Bokkel Huinink WW, van der Burg ME, van Oosterom AT, Willemse PH, Vermorken JB, *et al.* Long-term survival in ovarian cancer. Mature data from The Netherlands Joint Study Group for Ovarian Cancer. Eur J Cancer. 1991;27(11):1367–72.
4. Kartalou M, Essigmann JM. Mechanisms of resistance to cisplatin. Mutat Res. 2001;478(1-2):23–43.
5. Uchino H, Matsumura Y, Negishi T, Koizumi F, Hayashi T, Honda T, *et al.* Cisplatin-incorporating polymeric micelles (NC-6004) can reduce nephrotoxicity and neurotoxicity of cisplatin in rats. Br J Cancer. 2005;93(6):678–87.
6. Markman M, Rothman R, Hakes T, Reichman B, Hoskins W, Rubin S, *et al.* Second-line platinum therapy in patients with ovarian cancer previously treated with cisplatin. J Clin Oncol Off J Am Soc Clin Oncol. 1991;9(3):389–93.
7. Moghimi SM, Hunter AC, Murray JC. Nanomedicine: current status and future prospects. FASEB J Off Publ Fed Am Soc Exp Biol. 2005;19(3):311–30.
8. Duncan R. The dawning era of polymer therapeutics. Nat Rev Drug Discov. 2003;2(5):347–60.
9. Peer D, Karp JM, Hong S, Farokhzad OC, Margalit R, Langer R. Nanocarriers as an emerging platform for cancer therapy. Nat Nanotechnol. 2007;2(12):751–60.
10. Torchilin VP. Structure and design of polymeric surfactant-based drug delivery systems. J Control Release Off J Control Release Soc. 2001;73(2-3):137–72.
11. Oberoi HS, Nukolova NV, Kabanov AV, Bronich TK. Nanocarriers for delivery of platinum anticancer drugs. Adv Drug Deliv Rev. 2013;65(13-14):1667–85.
12. Stathopoulos GP. Liposomal cisplatin: a new cisplatin formulation. Anti-Cancer Drugs. 2010;21(8):732–6.
13. Zamboni WC, Gervais AC, Egorin MJ, Schellens JH, Zuhowski EG, Pluim D, *et al.* Systemic and tumor disposition of platinum after administration of cisplatin or STEALTH liposomal-cisplatin formulations (SPI-077 and SPI-077 B103) in a preclinical tumor model of melanoma. Cancer Chemother Pharmacol. 2004;53(4):329–36.
14. Ganta S, Singh A, Patel NR, Cacaccio J, Rawal YH, Davis BJ, *et al.* Development of EGFR-targeted nanoemulsion for imaging and novel platinum therapy of ovarian cancer. Pharm Res. 2014;31(9):2490–502.
15. Ganta S, Talekar M, Singh A, Coleman TP, Amiji MM. Nanoemulsions in translational research-opportunities and challenges in targeted cancer therapy. AAPS PharmSciTech. 2014;15(3):694–708.
16. Sarker DK. Engineering of nanoemulsions for drug delivery. Curr Drug Deliv. 2005;2(4):297–310.
17. Ganta S, Paxton JW, Baguley BC, Garg S. Pharmacokinetics and pharmacodynamics of chlorambucil delivered in parenteral emulsion. Int J Pharm. 2008;360(1–2):115–21.
18. Ganta S, Deshpande D, Korde A, Amiji M. A review of multifunctional nanoemulsion systems to overcome oral and CNS drug delivery barriers. Mol Membr Biol. 2010;27(7):260–73.
19. Ganta S, Sharma P, Paxton JW, Baguley BC, Garg S. Pharmacokinetics and pharmacodynamics of chlorambucil delivered in long-circulating nanoemulsion. J Drug Target. 2010;18(2):125–33.
20. Ganta S, Singh A, Rawal Y, Cacaccio J, Patel NR, Kulkarni P, *et al.* Formulation development of a novel targeted theranostic nanoemulsion of docetaxel to overcome multidrug resistance in ovarian cancer. Drug Deliv. 2014:1–13. doi:10.3109/10717544.2014.923068
21. Maeda H, Wu J, Sawa T, Matsumura Y, Hori K. Tumor vascular permeability and the EPR effect in macromolecular therapeutics: a review. J Control Release Off J Control Release Soc. 2000;65(1-2):271–84.
22. Ganta S, Amiji M. Coadministration of Paclitaxel and curcumin in nanoemulsion formulations to overcome multidrug resistance in tumor cells. Mol Pharm. 2009;6(3):928–39.
23. Talekar M, Ganta S, Singh A, Amiji M, Kendall J, Denny WA, *et al.* Phosphatidylinositol 3-kinase inhibitor (PIK75) containing surface functionalized nanoemulsion for enhanced drug delivery, cytotoxicity and pro-apoptotic activity in ovarian cancer cells. Pharm Res. 2012;29(10):2874–86.
24. Ganta S, Devalapally H, Amiji M. Curcumin enhances oral bioavailability and anti-tumor therapeutic efficacy of paclitaxel upon administration in nanoemulsion formulation. J Pharm Sci. 2010;99(11):4630–41.
25. Maeda M, Sasaki T, inventors; Sumitomo Pharmaceuticals Company Ltd, assignee. Liposoluble platinum (II) complex and preparation thereof patent 6,613,799 B1. 2003.
26. Nagaraja TN, Croxen RL, Panda S, Knight RA, Keenan KA, Brown SL, *et al.* Application of arsenazo III in the preparation and characterization of an albumin-linked, gadolinium-based macromolecular magnetic resonance contrast agent. J Neurosci Methods. 2006;157(2):238–45.
27. Zamboni WC, Gervais AC, Egorin MJ, Schellens JH, Hamburger DR, Delauter BJ, *et al.* Inter- and intratumoral disposition of platinum in solid tumors after administration of cisplatin. Clin Cancer Res. 2002;8(9):2992–9.
28. Jamieson ER, Jacobson MP, Barnes CM, Chow CS, Lippard SJ. Structural and kinetic studies of a cisplatin-modified DNA icosamer binding to HMG1 domain B. J Biol Chem. 1999;274(18):12346–54.
29. Wong E, Giandomenico CM. Current status of platinum-based antitumor drugs. Chem Rev. 1999;99(9):2451–66.
30. Wang D, Lippard SJ. Cellular processing of platinum anticancer drugs. Nat Rev Drug Discov. 2005;4(4):307–20.
31. Dhar S, Gu FX, Langer R, Farokhzad OC, Lippard SJ. Targeted delivery of cisplatin to prostate cancer cells by aptamer functionalized

Pt(IV) prodrug-PLGA-PEG nanoparticles. Proc Natl Acad Sci U S A. 2008;105(45):17356–61.
32. Dhar S, Kolishetti N, Lippard SJ, Farokhzad OC. Targeted delivery of a cisplatin prodrug for safer and more effective prostate cancer therapy in vivo. Proc Natl Acad Sci U S A. 2011;108(5):1850–5.
33. Paraskar AS, Soni S, Chin KT, Chaudhuri P, Muto KW, Berkowitz J, *et al.* Harnessing structure-activity relationship to engineer a cisplatin nanoparticle for enhanced antitumor efficacy. Proc Natl Acad Sci U S A. 2010;107(28):12435–40.
34. Stathopoulos GP, Boulikas T. Lipoplatin formulation review article. J Drug Delivery. 2012;2012:581363.
35. Harrington KJ, Lewanski CR, Northcote AD, Whittaker J, Wellbank H, Vile RG, *et al.* Phase I-II study of pegylated liposomal cisplatin (SPI-077) in patients with inoperable head and neck cancer. Ann Oncol Off J Eur Soc Med Oncol ESMO. 2001;12(4):493–6.
36. Cronin MT, Dearden JC, Duffy JC, Edwards R, Manga N, Worth AP, *et al.* The importance of hydrophobicity and electrophilicity descriptors in mechanistically-based QSARs for toxicological endpoints. SAR QSAR Environ Res. 2002;13(1):167–76.
37. Shen DW, Pouliot LM, Hall MD, Gottesman MM. Cisplatin resistance: a cellular self-defense mechanism resulting from multiple epigenetic and genetic changes. Pharmacol Rev. 2012;64(3):706–21.
38. Milane L, Duan Z, Amiji M. Development of EGFR-targeted polymer blend nanocarriers for combination paclitaxel/lonidamine delivery to treat multi-drug resistance in human breast and ovarian tumor cells. Mol Pharm. 2011;8(1):185–203.
39. Song S, Liu D, Peng J, Sun Y, Li Z, Gu JR, *et al.* Peptide ligand-mediated liposome distribution and targeting to EGFR expressing tumor in vivo. Int J Pharm. 2008;363(1-2):155–61.
40. Li Z, Zhao R, Wu X, Sun Y, Yao M, Li J, *et al.* Identification and characterization of a novel peptide ligand of epidermal growth factor receptor for targeted delivery of therapeutics. FASEB J Off Publ Fed Am Soc Exp Biol. 2005;19(14):1978–85.